Inorganic Chemistry

Article

High Spin and Spin-Crossover Two-Dimensional Coordination Polymers Containing Fe^{II}(tetrazol-2-yl)$_4$(solv)$_2$ (solv = Ethanol, Acetonitrile) Cores Linked by Flexible/Elastic Spacers

Agata Białońska and Robert Bronisz*

Faculty of Chemistry, University of Wrocław, F. Joliot-Curie 14, 50-383 Wrocław, Poland

1,6-Di(tetrazol-2-yl)hexane (**1, hbtz**) in the reaction with Fe(ClO$_4$)$_2$·6H$_2$O performed in acetonitrile or ethanol forms complexes {[Fe(**hbtz**)$_2$(CH$_3$CN)$_2$](ClO$_4$)$_2$}$_\infty$ (**2**) and {[Fe(**hbtz**)$_2$(C$_2$H$_5$OH)$_2$](ClO$_4$)$_2$}$_\infty$ (**3**), respectively. Both compounds crystallize in the triclinic system and $P\bar{1}$ space group. In **2** and **3** the basal plane of the coordination octahedron is formed by four tetrazole rings coordinated through N4 nitrogen atoms. The coordination spheres in **2** and **3** are completed by axially coordinated CH$_3$CN or C$_2$H$_5$OH molecules, respectively. In **2** and **3** ligand molecules bridge neighboring iron(II) ions in two directions resulting in two-dimensional (2D) networks. **3** is paramagnetic in the range 5−300 K whereas **2** undergoes the thermally induced HS $\rightleftharpoons$ LS transition (SCO) with $T_{1/2}{}^\uparrow = T_{1/2}{}^\downarrow$ = 128 K. Both complexes have very similar architecture with (4,4) network topology; however, the temperature dependence of ligand bridge parameters in **2** differs markedly from the ones observed for **3**. In **2** a lowering of temperature from 293 to 100 K causes a reduction of the distances between bridged iron(II) ions at 0.26 and 0.30 Å accompanied by the shortening of the distances between N4,N4′ donor atoms at about 0.04 and 0.09 Å indicating elasticity of the ligand molecules. In **3** at 250 K iron(II) ions are linked by ordered and disordered over two positions **hbtz** bridges. Cooling to 100 K involves a shortening of Fe$\cdots$Fe and N4$\cdots$N4′ distances of the ordered bridge at 0.09 and 0.07 Å, respectively. The previously disordered bridge is ordered at 100 K, and only one conformer is present. In this case conformational changes enable a reduction of Fe$\cdots$Fe and N4$\cdots$N4′ distances at about 0.14 and 0.14 Å, respectively.

Introduction

The design and construction of coordination networks attract considerable attention because of the interesting properties and possible applications of such materials.[1] Preparation of coordination polymers through self-assembly process requires an application of ligand systems with specified structure and coordination properties of donor groups. Among donors, utilized for preparation of ligand systems useful for construction of coordination networks, tetrazoles exhibit a large versatility of the coordination modes depending on the position of a substituent in the ring. 5-Substituted derivatives can act as monodentate ligands although in most cases they bridge metal ions forming coordination networks.[2] Contrary to 5-substituted tetrazoles their 1-substituted regio-isomers usually coordinate monodentately with metal ions through an *exo* located N4 nitrogen atom of the ring giving molecular species.[3] Mono 1-substituted tetrazoles (1RTz)

can be components of the polynuclear complexes but in this type of systems other ligands act as bridging units.[4] A construction of coordination networks based on metal ions homoleptically surrounded by 1-substituted tetrazoles demands an application of ligand systems containing at least two tetrazole rings in the molecule.[5] In this way spin-crossover polymeric materials based exclusively on tetrazole rings as donor groups were prepared.[6] Coordination networks

*To whom correspondence should be addressed. E-mail: bron@wchuwr.pl.

(1) Kitagawa, S.; Kitaura, R.; Noro, S.-I. *Angew. Chem., Int. Ed.* **2004,** *43,* 2334–2375.
(2) Zhao, H.; Qu, Z.-R.; Ye, H.-Y.; Xiong, R.-G. *Chem. Soc. Rev.* **2008,** *37,* 84–100.
(3) Gaponik, P. N.; Voitekhovich, S. V.; Ivashkevich, O. A. *Russ. Chem. Rev.* **2006,** *75,* 507–539.

(4) (a) Virovets, A. V.; Podberezskaya, N. V.; Lavrenova, L. G. *Acta Crystallogr.* **1995,** *C51,* 1084–1087. (b) Ivashkevich, D. O.; Lyakhov, A. S.; Gaponik, P. N.; Bogatikov, A. N.; Govorova, A. A. *Acta Crystallogr.* **2001,** *E57,* m335–m337. (c) Ivashkevich, D. O.; Degtyarik, M. M.; Gaponik, P. N.; Lyakhov, A. S. *Acta Crystallogr.* **2002,** *C58,* m288–m289. (d) Ivashkevich, D. O.; Lyakhov, A. S.; Degtyarik, M. M.; Gaponik, P. N. *Acta Crystallogr.* **2003,** *E59,* m14–m16. (e) Ivashkevich, D. O.; Lyakhov, A. S.; Degtyarik, M. M.; Gaponik, P. N. *Acta Crystallogr.* **2004,** *C60,* m368–m370. (f) Ivashkevich, D. O.; Lyakhov, A. S.; Degtyarik, M. M.; Gaponik, P. N. *Acta Crystallogr.* **2005,** *E61,* m394–m396. (g) Stassen, A. F.; Kooijman, H.; Spek, A. L.; de Jongh, L. J.; Haasnoot, J. G.; Reedijk, J. *Inorg. Chem.* **2002,** *41,* 6468–6473. (h) Shvedenkov, Y. G.; Virovets, A. V.; Lavrenova, L. G. *Russ. Chem. Bull., Int. Ed.* **2003,** *6,* 1281–1285. (i) Shvedenkov, Y.; Bushuev, M.; Romanenko, G.; Lavrenova, L.; Ikorskii, V.; Gaponik, P.; Larionov, S. *Eur. J. Inorg. Chem.* **2005,** 1678–1682.
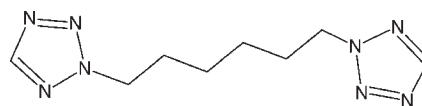(5) (a) Liu, P.-P.; Cheng, A.-L.; Liu, N.; Sun, W.-W.; Gao, E.-Q. *Chem. Mater.* **2007,** *19,* 2724–2726. (b) van Koningsbruggen, P. J.; Garcia, Y.; Bravic, G.; Chasseau, D.; Kahn, O. *Inorg. Chim. Acta* **2001,** *326,* 101–105.
(6) (a) van Koningsbruggen, P. J. *Top. Curr. Chem.* **2004,** *233,* 123–149. (b) Garcia, Y.; Niel, V.; Munoz, M. C.; Real, J. A. *Top. Curr. Chem.* **2004,** *233,* 229–257.

based on bis- and tristetrazole-type ligands exhibit a diversification of their architectures. Depending on the nature of a spacer linking the rings, iron(II) complexes were isolated as 1D,[7] 2D,[8] and 3D[9] nets. In these systems a coordination environment of the Fe(II) ions is very similar to that observed in monomeric [Fe(1RTz)$_6$]X$_2$ complexes.[10] Investigations of coordination properties of 2-substituted tetrazoles revealed that this third type of tetrazole based donor group is suitable for preparation of iron(II) coordination polymers exhibiting the spin-crossover phenomenon.[11] Also here six 2-substituted tetrazoles form the first coordination sphere of the iron(II) ions coordinating through the N4 nitrogen atom of the ring. Such a polymeric approach was applied to the preparation of other groups of spin crossover coordination networks involving: 1,2,4-triazole ring, cyanometallate anions and bis-(pyridyl) moieties as bridging units.[6b,12]

Taking into account that the number of bisazole-type ligands containing a simple alkyl spacer is limited, we have decided to expand our studies on bitopic ligand systems.[13] Recently, within the framework of this investigation, we have reported that 2-hydroxy-1-(tetrazol-1-yl)-3-(tetrazol-2-yl)-propane (**12pbtzOH**) in the reaction with Fe(ClO$_4$)$_2$·6H$_2$O performed in acetonitrile forms a 1D coordination polymer {[Fe(**12pbtzOH**)$_2$(CH$_3$CN)$_2$](ClO$_4$)$_2$·2CH$_3$CN}$_\infty$ exhibiting

(7) (a) Schweifer, J.; Weinberger, P.; Mereiter, K.; Boca, M.; Reichl, C.; Wiesinger, G.; Hilscher, G.; van Koningsbruggen, P. J.; Kooijman, H.; Grunert, M.; Linert, W. *Inorg. Chim. Acta* **2002**, *339*, 297–306. (b) van Koningsbruggen, P. J.; Garcia, Y.; Fournès, L.; Kooijman, H.; Spek, A. L.; Haasnoot, J. G.; Moscovici, J.; Provost, K.; Michalowicz, A.; Renz, F.; Gütlich, P. *Inorg. Chem.* **2000**, *39*, 1891–1900. (c) Quesada, M.; Kooijman, H.; Gamez, P.; Costa, J. S.; van Koningsbruggen, P. J.; Weinberger, P.; Reissner, M.; Spek, A. L.; Haasnoot, J. G.; Reedijk, J. *Dalton Trans.* **2007**, 5434–5440. (d) Quesada, M.; Prins, F.; Bill, E.; Kooijman, H.; Gamez, P.; Roubeau, O.; Spek, A. L.; Haasnoot, J. G.; Reedijk, J. *Chem.—Eur. J.* **2008**, *14*, 8486–8499.

(8) (a) Quesada, M.; Prins, F.; Roubeau, O.; Gamez, P.; Teat, S. J.; van Koningsbruggen, P. J.; Haasnoot, J. G.; Reedijk, J. *Inorg. Chim. Acta* **2007**, *360*, 3787–3796. (b) Bronisz, R.; Ciunik, Z.; Drabent, K.; Rudolf, M. F. *Conf. Proc., ICAME-95* **1996**, *50*, 15–18.

(9) (a) Grunert, C. M.; Schweifer, J.; Weinberger, P.; Linert, W.; Mereiter, K.; Hilscher, G.; Müller, M.; Wiesinger, G.; van Koningsbruggen, P. J. *Inorg. Chem.* **2004**, *43*, 155–165. (b) Bartel, M.; Absmeier, A.; Jameson, G. N. L; Werner, F.; Kato, K.; Takata, M.; Boca, R.; Hasegawa, M.; Mereiter, K.; Caneschi, A.; Linert, W. *Inorg. Chem.* **2007**, *46*, 4220–4229. (c) van Koningsbruggen, P. J.; Garcia, Y.; Kooijman, H.; Spek, A. L.; Haasnoot, J. G.; Kahn, O.; Linares, J.; Codjovi, E.; Varret, F. *J. Chem. Soc., Dalton Trans.* **2001**, 466–471.

(10) (a) Wiehl, L. *Acta Crystallogr.* **1993**, *B49*, 289–303. (b) Hinek, R.; Spiering, H.; Shollmeyer, D.; Gütlich, P.; Hauser, A. *Chem.—Eur. J.* **1996**, *11*, 1427–1434. (c) Jeftic, J.; Hinek, R.; Capelli, S. C.; Hauser, A. *Inorg. Chem.* **1997**, *36*, 3080–3087. (d) Dova, E.; Peschar, R.; Sakata, M.; Kato, K.; Schenk, H. *Chem.—Eur. J.* **2006**, *12*, 5043–5052. (e) Dova, E.; Stassen, A. F.; Driessen, R. A. J.; Sonneveld, E.; Goubitz, K.; Peschar, R.; Haasnoot, J. G.; Reedijk, J.; Schenk, H. *Acta Crystallogr.* **2001**, *B57*, 531–538. (f) Dova, E.; Peschar, R.; Takata, M.; Nishibori, E.; Schenk, H.; Stassen, A. F.; Haasnoot, J. G. *Chem.—Eur. J.* **2005**, *11*, 5855–5865. (g) Dova, E.; Peschar, R.; Sakata, M.; Kato, K.; Stassen, A. F.; Schenk, H.; Haasnoot, J. G. *Acta Crystallogr.* **2004**, *B60*, 528–538. (h) Soliman, A. A.; Khattab, M. M.; Reissner, M.; Weinberger, P.; Werner, F.; Linert, W. *Inorg. Chim. Acta* **2007**, *60*, 3987–3996. (i) Hassan, N.; Weinberger, P.; Mereiter, K.; Werner, F.; Molnar, G.; Bousseksou, A.; Valtiner, M.; Linert, W. *Inorg. Chim. Acta* **2008**, *361*, 1291–1297.

(11) Bronisz, R. *Inorg. Chem.* **2007**, *46*, 6733–6739.

(12) (a) Real, J. A.; Gaspar, A. B.; Niel, V.; Munoz, M. C. *Coord. Chem. Rev.* **2003**, *236*, 121–141. (b) Real, J. A.; Gaspar, A. B.; Munoz, M. C. *Dalton Trans.* **2005**, 2062–2079. (c) Murray, K. S. *Eur. J. Inorg. Chem.* **2008**, 3101–3121. (d) Dîrtu, M. M.; Rotaru, A.; Gillard, D.; Linares, J.; Codjovi, E.; Tinant, B.; Garcia, Y. *Inorg. Chem.* **2009**, *48*, 7838–7852. (e) Matouzenko, G. S.; Perrin, M.; Le Guennic, B.; Genre, C.; Molnar, G.; Bousseksouc, A.; Borshcha, S. A. *Dalton Trans.* **2007**, 934–942. (f) Martinez, V.; Gaspar, A. B.; Munoz, M. C.; Bukin, G. V.; Levchenko, G.; Real, J. A. *Chem.—Eur. J.* **2009**, *15*, 10960–10971. (g) Agustí, G.; Munoz, M. C.; Gaspar, A. B.; Real, J. A. *Inorg. Chem.* **2009**, *48*, 3371–3381 and references therein.

(13) Białońska, A.; Bronisz, R. *Tetrahedron* **2008**, *64*, 9771–9779.

Scheme 1

a HS$\leftrightarrows$LS transition.[14] An unprecedented feature of this mono tetrazole based complex is the presence of the spin crossover centers of composition Fe(tetrazol-1-yl-κN^4)$_2$-(tetrazol-2-yl-κN^4)$_2$(CH$_3$CN)$_2$. On the other hand a synthesis between an isomeric ligand containing only tetrazol-1-yl donors, that is, 2-hydroxy-1,3-di(tetrazol-1-yl)propane, and Fe(BF$_4$)$_2$·6H$_2$O performed in acetonitrile leads to formation of a 2D spin crossover system in which iron(II) ions are typically surrounded by six 1-substituted tetrazole rings.[8a] Because other bis(tetrazol-1-yl)alkanes form with iron(II) salts homoleptic complexes, a question concerning a role of 2-substituted tetrazole ring on a formation of heteroleptic species arises.

Continuing our investigations concerning an application of flexible/elastic bisazole-type ligands for preparation of spin-crossover polymeric materials, we have synthesized novel ligand with long alkyl spacer, 1,6-di(tetrazol-2-yl)-hexane (**hbtz**, Scheme 1).

Investigations of this ligand system, containing exclusively tetrazol-2-yl as donor group, revealed its ability to form coordination polymers containing Fe(tetrazol-2-yl-κN^4)$_4$-(solv)$_2$ cores (solv = CH$_3$CN, C$_2$H$_5$OH). Obtained complexes differ from each other in their magnetic properties. Whereas {[Fe(**hbtz**)$_2$(CH$_3$CN)$_2$](ClO$_4$)$_2$}$_\infty$ (**2**) exhibits thermally induced spin crossover, the {[Fe(**hbtz**)$_2$(C$_2$H$_5$OH)$_2$]-(ClO$_4$)$_2$}$_\infty$ (**3**) remains paramagnetic in the range 5−300 K. In this paper we report on synthesis of **hbtz** and products of reactions between **hbtz** and Fe(ClO$_4$)$_2$·6H$_2$O performed in acetonitrile and ethanol. Results of X-ray diffraction studies of **2** carried out at 293, 250, 200, 150, 125, and 100 K and **3** at 250 and 100 K and the magnetic measurements for both compounds are presented.

Experimental Section

Materials and Methods. Infrared spectra were recorded with the Bruker IFS66 IR FTIR spectrometer in the range 50−4000 cm^{-1} as KBr pellets (compound **1**) or in nujol mulls (**2** and **3**). Elemental analyses for carbon, hydrogen, and nitrogen were performed on a Perkin-Elmer 240C analyzer. Temperature measurements of the magnetic susceptibility were carried out with a Quantum Design SQUID magnetometer in the 5−300 K temperature range operating at 1 T. Magnetic data were corrected for the diamagnetic contributions, which were estimated from Pascal's constants. Ethanol was dried by a distillation over a magnesium ethanolate. Acetonitrile was dried by a distillation over calcium hydride. 1H,2,3,4-tetrazole was prepared using a known procedure.[15] Iron(II) perchlorate hexahydrate purchased from Aldrich was used. The other commercially available reagents were used without further purification. *Caution! Even though no problems were encountered it is worth to mention that complexes containing perchlorates are potentially explosive and should be synthesized and handled with care.*

Synthesis of 1,6-Di(tetrazol-2-yl)hexane (1). A solution of NaOH (0.10 mol, 4.0 g) in water (20 mL) was added in a few portions to 1H,2,3,4-tetrazole (0.10 mol, 7.0 g) dissolved in water (20 mL). Then, water was removed using a rotary

(14) Białońska, A.; Bronisz, R.; Weselski, M. *Inorg. Chem.* **2008**, *47*, 4436–4438.

(15) Kamiya, T.; Saito, Y. *Ger. Offen.* **1973**, German Patent no. 2147023.

Table 1. Crystallographic Data for **2** and **3**

	2						**3**	
formula	$C_{20}H_{34}Cl_2FeN_{18}O_8$						$C_{20}H_{40}Cl_2FeN_{16}O_{10}$	
M_w	781.40						791.43	
T (K)	293 K	250 K	200 K	150 K	125 K	100 K	250 K	100 K
λ (Å)	0.71073						0.71073	
Space group	$P\bar{1}$						$P\bar{1}$	
a (Å)	9.526(2)	9.532(2)	9.548(2)	9.561(2)	9.530(2)	9.491(2)	9.860(2)	9.847(2)
b (Å)	9.542(3)	9.496(2)	9.436(2)	9.374(2)	9.359(2)	9.331(2)	9.314(2)	9.220(2)
c (Å)	11.736(3)	11.693(3)	11.635(3)	11.565(3)	11.518(3)	11.406(3)	11.845(3)	11.772(3)
a (deg)	69.01(3)	69.36(3)	69.84(3)	70.44(3)	70.28(3)	70.24(3)	69.54(3)	69.50(3)
b (deg)	89.15(3)	89.50(3)	89.99(3)	90.54(3)	90.61(3)	90.82(3)	89.25(3)	89.56(3)
γ (deg)	65.47(4)	65.56(4)	65.69(4)	65.86(4)	65.87(4)	65.91(4)	60.93(4)	60.68(4)
V (Å^3)	894.8(4)	890.0(3)	884.4(3)	878.3(3)	869.3(3)	854.1(3)	874.3(6)	855.1(6)
Z	1						1	
D_c (Mg·m^{-3})	1.450	1.458	1.467	1.477	1.493	1.519	1.503	1.537
μ (mm^{-1})	0.638	0.642	0.646	0.650	0.657	0.669	0.656	0.671
$R1$ $(I > 2\sigma_I)^a$	0.0601	0.0525	0.0447	0.0413	0.0413	0.056	0.0376	0.0304
wR^2 $(I > 2\sigma_I)^b$	0.1037	0.0993	0.0665	0.0672	0.0783	0.1170	0.0903	0.0753

^{a} $R1 = \sum||F_o| - |F_c||/\sum|F_o|$. ^{b} $wR^2 = [\sum w(F_o{}^2 - F_c{}^2)^2/\sum w(F_o{}^2)^2]^{1/2}$.

evaporator, and the obtained solid matter was dehydrated by an aseotropic distillation with three portions (each 100 mL) of absolute ethanol. To the whole amount of obtained sodium tetrazolate suspended in acetonitrile (100 mL) was added 1, 6-dibromohexane (0.04 mol, 6.1 mL) dissolved in acetonitrile (25 mL). The reaction mixture was stirred and refluxed for 4 days. Then the NaBr was filtered off, and acetonitrile was removed under reduced pressure. An obtained residue was dissolved in water (300 mL) and then extracted with pentane (300 mL) and with CCl_4 (10 × 150 mL). The combined CCl_4 extracts were dried over anhydrous Na_2SO_4. A crude product was obtained after removing of CCl_4 under reduced pressure. An obtained solid mass was dissolved in boiling water (200 mL). Crystallization of the product starts after seeding of the cooled solution. After recrystallization from water (110 mL) colorless needles were filtered off and dried over sodium hydroxide. Yield 12.5% (1.12 g). Anal. found: C, 43.4; H, 6.3; N, 50.6%. Calcd for $C_8H_{14}N_8$ (M_w = 222.25): C, 43.2; H, 6.4; N, 50.4. IR(KBr): 3134(s), 3008(s), 2946(s), 2868(s), 1785(w), 1631(w), 1469(s), 1452(m), 1384(w), 1376(w), 1356(s), 1278(s), 1254(m), 1180(m), 1145(m), 1101(m), 1082(w), 1034(s), 1012(m), 976(w), 896(m), 798(w), 769(m), 763(m, sh), 750(m), 709(m), 694(m) cm^{-1}. ^{1}HNMR (500 MHz, CD_3CN, 298 K) δ: 8.55 (s, 2H, C*H* of tetrazol-2-yl), 4.60 (t, 4H, $-CH_2-CH_2-CH_2$-tetrazol-2-yl, ^3J = 6.0 Hz), 1.94 (m, 4H, $-CH_2-CH_2$-CH_2-tetrazol-2-yl), 1.29 (m, 4H, $-CH_2-CH_2-CH_2$-tetrazol-2-yl) ppm. ^{13}C NMR (500 MHz, CD_3CN, 298 K) δ: 153.8, 53.6, 29.5, 26.2 ppm.

Synthesis of {[Fe(hbtz)$_2$(CH$_3$CN)$_2$](ClO$_4$)$_2$}$_\infty$ (2). To the solution of **hbtz** (0.30 mmol, 0.0666 g) in dry acetonitrile (2.0 mL) was added solid Fe(ClO$_4$)$_2$·6H$_2$O (0.15 mmol, 0.0544 g). The resultant colorless solution was concentrated to the volume of about 0.5 mL and next was left under nitrogen atmosphere in a closed Schlenk flask. After 3 days colorless crystals were filtered off and dried in the stream of nitrogen. Yield 56% (0.066 g). Anal. found: C, 30.7; H, 4.5; N, 32.3.

Calcd for FeC$_{20}$H$_{34}$N$_{18}$Cl$_2$O$_8$ (M_w = 781.35): C, 30.7; H, 4.4; N, 32.3%. IR(nujol): 3144(m), 2924(s, br), 2308(m), 2280(m), 2022(w), 1819(w), 1466(s), 1446(s, sh), 1377(s), 1365(s, sh), 1305(m), 1265(w), 1257(w, sh), 1188(m), 1151(s, sh), 1097(s), 1044(s, sh), 1029(s, sh), 994(m, sh), 934(w), 915(m), 859(w), 785(w), 745(w), 723(w), 714(w), 699(m), 665(m), 624(s), 531(w), 484(w) cm^{-1}.

Synthesis of {[Fe(hbtz)$_2$(C$_2$H$_5$OH)$_2$](ClO$_4$)$_2$}$_\infty$ (3). The synthesis was performed according the procedure described for **2** using 4.0 mL of absolute ethanol instead of acetonitrile. Yield 40% (0.048 g). Anal.found: C, 30.0; H, 4.6; N, 28.5. Calcd for FeC$_{20}$H$_{40}$N$_{16}$Cl$_2$O$_{10}$ (M_w = 791.38): C, 30.4; H, 5.1.; N, 28.3%. IR(nujol): 3294(m, br), 3147(m), 2925(s, br), 1464(s), 1377(s), 1303(m), 1188(m), 1147(s, sh), 1105(s), 1045(s, sh), 1026(s, sh),

995(m), 931(w), 918(w), 900(w), 873(w), 805(w), 747(w), 735(w), 717(w), 698(m), 660(w), 622(m), 528(w), 479(w), 462(w) cm^{-1}.

X-ray Data Collection and Structure Determination. The crystals of **2** and **3** suitable for X-ray measurements were selected from the crystalline product obtained according with the aforementioned synthesis procedure of the complexes. Crystals were coated by a layer of inert oil and immediately transferred to the stream of nitrogen of the diffractometer. Crystal data and refinement details for **2** and **3** are listed in Table 1. The measurements were performed at 293, 250, 200, 150, 125, and 100 K for **2** and at 250 and 100 K for **3**. All the measurements were performed using an Oxford Cryosystem device on a Kuma KM4CCD κ-axis diffractometer with graphite-monochromated Mo Kα radiation. The data were corrected for Lorentz and polarization effects. Analytical absorption correction was applied. Data reduction and analysis were carried out with the Oxford Diffraction (Poland) Sp. z o.o. (formerly Kuma Diffraction Wroclaw, Poland) programs. The structures were solved by direct methods (program SHELXS97[16]) and refined by the full-matrix least-squares method on all F^2 data using the SHELXL97[17] program.

Non-hydrogen atoms were refined with anisotropic displacement parameters. The occupancy factor for the disordered anion in **2** and for the disordered anion as well as solvent and ligand molecules in **3** were refined. Atoms, for which values of occupancy factor are less than 0.5, were refined using ISOR restrain. All H atoms in **2** and **3** were found in $\Delta\rho$ maps or placed at calculated positions. Before the last cycle of refinement, all H atoms were fixed and were allowed to ride on their parent atoms.

Results and Discussion

Synthesis and General Characterization. Synthesis of mono 2-substituted tetrazoles as distinct from their 1-substituted regioisomers is not regioselective. There are only a few syntheses leading exclusively to formation of mono 2-substituted products.[18] Usually mono 2-substituted

(16) Sheldrick, G. M. *SHELXS97, program for solution of crystal structures*; University of Göttingen: Göttingen, Germany, 1997.

(17) Sheldrick, G. M. *SHELXL97, program for crystal structure refinement*; University of Göttingen: Göttingen, Germany, 1997.

(18) (a) Koren, A. O.; Gaponik, P. N. *Khim. Geterotsik. Soedin.* **1990**, *12*, 1643–1647. (b) Shchirobokov, I. Y.; Sachivko, A. V.; Tverdokhlebov, V. P.; Ostrovskii, V. A.; Tselinskii, I. V.; Koldobskii, G. I. *Zh. Org. Khim.* **1986**, *22*, 1763–1768. (c) Koren, A. O.; Gaponik, P. N.; Ostrovskii, V. A. *Int. J. Chem. Kinet.* **1993**, *25*, 1043–1051. (d) Koren, A. O.; Gaponik, P. N.; Ostrovskii, V. A. *Int. J. Chem. Kinet.* **1995**, *27*, 919–924. (e) Voitekhovich, S. V.; Gaponik, P. N.; Koren, A. O. *Mendeleev Commun.* **1997**, *7*, 41–42.

derivatives are prepared by alkylation of tetrazole with suitable halogen derivatives. However comparable amounts of 1- and 2-substituted tetrazoles are formed. In this way both monodentate 2-substituted tetrazoles and bidentate 1,ω-di(tetrazol-2-yl)alkanes can be obtained. The novel bidentate ligand with long alkyl chain 1,6-di(tetrazol-2-yl)hexane was synthesized in the reaction of sodium tetrazolate with the 1,6-dibromohexane. A synthesis yield of 12.5% is caused by formation of two other regioisomers (1,6-di(tetrazol-1-yl)hexane and 1-(tetrazol-1-yl)-6-(tetrazol-2-yl)hexane) and is comparable to the yields obtained for other members of this ligand family. **Hbtz** crystallizes as stable colorless crystals soluble in CH_3CN, CH_3OH, and CH_2Cl_2.

2-Substituted tetrazoles easily form heteroleptic complexes with copper(II) chloride.[19] In the absence of the potentially coordinating halides, formation of complexes with metal(II) ions surrounded by six tetrazole rings M(tetrazol-2-yl)$_6$ where M = Fe(II), Ni(II), Cu(II), Zn(II)[11,20] or systems with first coordination sphere of composition Cu(tetrazol-2-yl)$_4$(CH$_3$OH)$_2$[20c] has been observed. There are also known complexes in which tetrazol-2-yl act as bridging units.[21] It is worthy of mention that also 1-substituted tetrazoles exhibit an ability to form homo-[10,22] and heteroleptic[23] complexes. Recently we have prepared a complex based on a mixed ligand system {[Fe(**12pbtzOH**)$_2$(CH$_3$CN)$_2$](ClO$_4$)$_2$·2CH$_3$CN}$_\infty$ in which, besides both 1- and 2-substituted tetrazole rings, acetonitrile molecules form a coordination sphere of iron(II). Hence, considering the possibility of formation of homo- and heteroleptic complexes, we have performed syntheses

(19) (a) Lyakhov, A. S.; Gaponik, P. N.; Degtyarik, M. M.; Matulis, V. E.; Matulis, V. E.; Ivashkevich, L. S. *Acta Crystallogr.* **2003**, *C59*, m90–m92. (b) Lyakhov, A. S.; Gaponik, P. N.; Degtyarik, M. M.; Ivashkevich, L. S. *Acta Crystallogr.* **2003**, *E59*, m38–m40. (c) Lyakhov, A. S.; Gaponik, P. N.; Degtyarik, M. M.; Ivashkevich, L. S. *Acta Crystallogr.* **2005**, *E61*, m183–m186.

(20) (a) van den Heuvel, E. J.; Franke, P. L.; Verschoor, G. C.; Zuur, A. P. *Acta Crystallogr.* **1983**, *C39*, 337–339. (b) Bronisz, R. *Inorg. Chim. Acta* **2002**, *340*, 215–220. (c) Bronisz, R. *Inorg. Chim. Acta* **2004**, *357*, 396–404. (d) Bronisz, R. *Eur. J. Inorg. Chem.* **2004**, 3688–3695.

(21) (a) Gaponik, P. N.; Degtyarik, M. M.; Lyakhov, A. S.; Matulis, V. E.; Ivashkevich, O. A.; Quesada, M.; Reedijk, J. *Inorg. Chim. Acta* **2005**, *358*, 3949–3957. (b) Lyakhov, A. S.; Gaponik, P. N.; Degtyarik, M. M.; Ivashkevich, L. S. *Acta Crystallogr.* **2003**, *C59*, m204–m206. (c) Lyakhov, A. S.; Degtyarik, M. M.; Ivashkevich, L. S.; Gaponik, P. N. *Acta Crystallogr.* **2005**, *C61*, m158–m160.

(22) (a) Stassen, A. F.; Kooijman, H.; Spek, A. L.; Haasnoot, J. G.; Reedijk, J. *J. Chem. Crystallogr.* **2001**, *31*, 307–314. (b) Stassen, A. F.; Roubeau, O.; Gramage, I. F.; Linares, J. *Polyhedron* **2001**, *20*, 1699–1707. (c) Yamaura, J.-I.; Kato, R. *Phys. Rev.* **1998**, *B58*, 14098–14101. (d) Wijnands, P. E. M.; Wood, J. S.; Reedijk, J.; Maaskant, W. J. A. *Inorg. Chem.* **1996**, *35*, 1214–1222.

(23) (a) Virovets, A. V.; Podberezskaya, N. V.; Lavrenova, L. G. *Acta Crystallogr.* **1995**, *C51*, 1084–1087. (b) Ivashkevich, D. O.; Lyakhov, A. S.; Gaponik, P. N.; Bogatikov, A. N.; Govorova, A. A. *Acta Crystallogr.* **2001**, *E57*, m335–m337. (c) Ivashkevich, D. O.; Degtyarik, M. M.; Gaponik, P. N.; Lyakhov, A. S. *Acta Crystallogr.* **2002**, *C58*, m288–m289. (d) Ivashkevich, D. O.; Lyakhov, A. S.; Degtyarik, M. M.; Gaponik, P. N. *Acta Crystallogr.* **2003**, *E59*, m14–m16. (e) Ivashkevich, L. S.; Lyakhov, A. S.; Degtyarik, M. M.; Gaponik, P. N. *Acta Crystallogr.* **2005**, *E61*, m394–m396. (f) Zhanga, S.-M.; Du, J.-L. *Acta Crystallogr.* **2007**, *E63*, m3139. (g) Ivashkevich, L. S.; Lyakhov, A. S.; Serebryanskaya, T. V.; Gaponik, P. N. *Acta Crystallogr.* **2008**, *E64*, m1044–m1045. (h) Shvedenkov, Y.; Bushuev, M.; Romanenko, Lavrenova, G. L.; Ikorskii, V.; Gaponik, P.; Larionov, S. *Eur. J. Inorg. Chem.* **2005**, 1678–1682. (i) Stassen, A. F.; Kooijman, H.; Spek, A. L.; de Jongh, L. J.; Haasnoot, J. G.; Reedijk, J. *Inorg. Chem.* **2002**, *41*, 6468–6473. (j) Liu, P.-P.; Cheng, A.-L.; Liu, N.; Sun, W.-W.; Gao, E.-Q. *Chem. Mater.* **2007**, *19*, 2724–2726. (k) Yu, Q.; Zhang, X.; Bian, H.; Liang, H.; Zhao, B.; Yan, S.; Liao, D. *Cryst. Growth Des.* **2008**, *8*, 1140–1146.
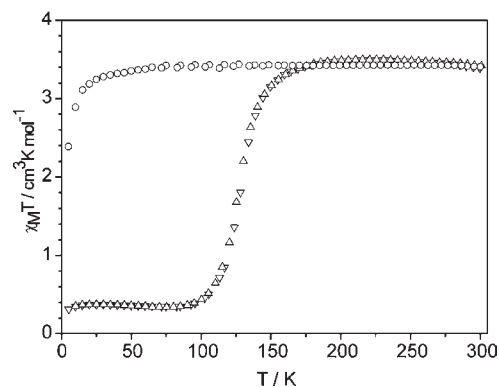

Figure 1. $\chi_M T$ vs T plots for **2** in cooling (open down triangles) and warming (open up triangles) modes and for **3** in cooling (open circles) mode.
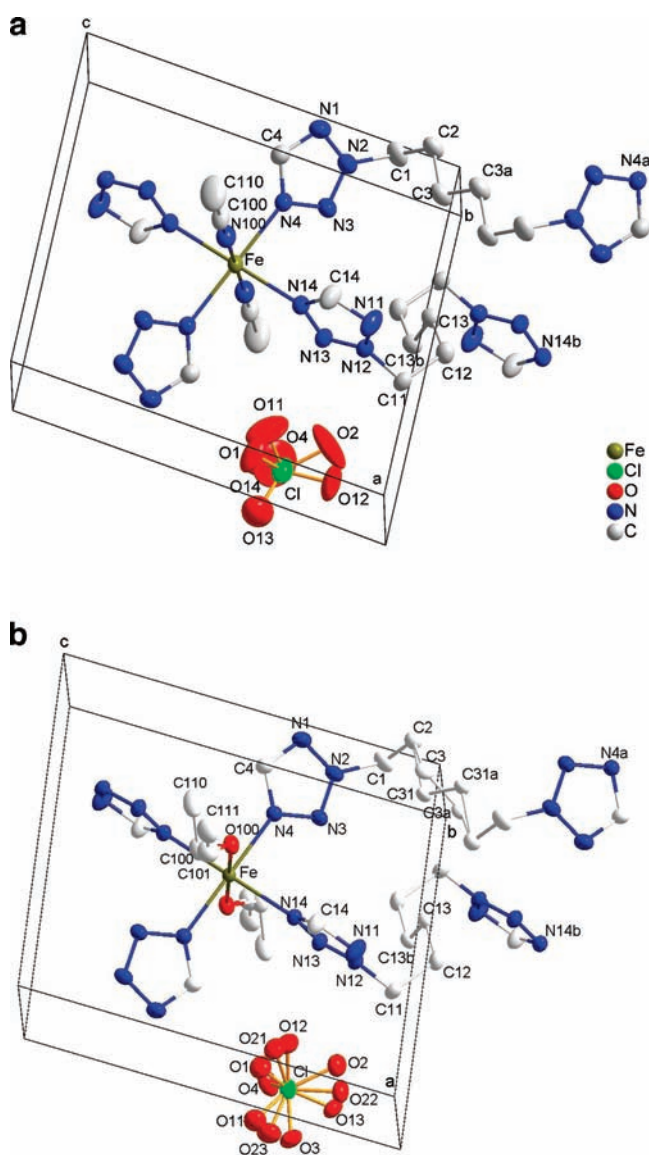

Figure 2. Comparison of the coordination environments and the conformation differences between **2** (a) and **3** (b) (thermal ellipsoids at the 30% probability level), showing the labeling scheme of atoms employed. Hydrogen atoms were omitted for clarity. Symmetry operations: a = −x, 1 − y, −z; b = 1 − x, −y, −z.

between **hbtz** and Fe(ClO$_4$)$_2$·6H$_2$O in various ligand to metal molar ratios. {[Fe(**hbtz**)$_2$(CH$_3$CN)$_2$](ClO$_4$)$_2$}$_\infty$ (**2**) was

Table 2. Selected Fe−N Distances (Å), N−Fe−N Angles (deg), Torsion Angles (deg), Fe···Fe, N4,N4′, N2,N2′, and Fe···Cl Interatomic Distances (Å) for **2** at 293, 250, 200, 150, 125, and 100 K and for **3** at 250 and 100 K[a]

	2						**3**	
	293 K	250 K	200 K	150 K	125 K	100 K	250 K	100 K
Fe−N4	2.166(3)	2.165(3)	2.159(3)	2.140(3)	2.080(3)	2.000(3)	2.189(2)	2.191(2)
Fe−N14	2.189(3)	2.188(3)	2.175(3)	2.158(3)	2.094(3)	2.011(3)	2.207(2)	2.195(2)
Fe−X100	2.162(4)	2.162(3)	2.160(3)	2.136(3)	2.061(3)	1.953(3)	2.098(2)	2.089(2)
N4−Fe−N14	88.0(1)	88.0(1)	88.1(1)	88.2(1)	88.2(1)	88.2(1)	90.74(7)	90.75(6)
N4−Fe−N14[b]	92.0(1)	92.0(1)	91.9(1)	91.8(2)	91.8(1)	91.8(1)	89.26(7)	89.25(6)
N4−Fe−X100	90.6(2)	90.8(1)	90.8(1)	90.9(1)	90.7(1)	90.7(1)	93.84(8)	93.62(7)
N4−Fe−X100[b]	89.4(2)	89.2(1)	89.2(1)	89.1(1)	89.3(1)	89.3(1)	86.16(8)	86.38(7)
N14−Fe−X100	90.4(1)	90.1(1)	90.1(1)	89.9(1)	89.6(1)	89.6(1)	92.17(7)	91.77(6)
N14−Fe−X100[b]	89.6(1)	89.9(1)	89.9(1)	90.1(1)	90.4(1)	90.4(1)	87.83(7)	88.23(6)
N11−N12−C11−C12	−73.3(4)	−72.7(4)	−72.6(4)	−72.0(4)	−72.4(3)	−71.9(4)	−85.4(3)	−84.26(19)
N12−C11−C12−C13	−60.2(4)	−60.5(4)	−60.3(3)	−59.9(3)	−59.5(3)	−60.0(3)	−62.0(3)	−60.93(19)
C11−C12−C13−C13[c]	−64.8(5)	−63.6(5)	−63.4(4)	−63.4(4)	−64.2(4)	−64.0(4)	−63.2(3)	−62.1(2)
N1−N2−C1−C2	72.3(5)	72.0(4)	72.6(4)	72.8(4)	72.4(3)	71.6(4)	70.1(3)	69.63(19)
N2−C1−C2−C3	67.1(5)	66.3(4)	65.9(4)	64.5(4)	63.4(3)	63.0(4)	64.0(3)	66.55(18)
N2−C1−C2−C31							81.4(5)	
C1−C2−C3−C3[d]	175.7(4)	175.6(4)	175.7(4)	174.7(3)	175.0(3)	175.2(3)	71.6(4)	71.0(2)
C1−C2−C31−C31[d]							170.1(13)	
Fe···Fe[e]	12.928(8)	12.904(8)	12.875(8)	12.847(8)	12.770(8)	12.663(8)	12.687(8)	12.546(8)
Fe···Fe[f]	11.736(3)	11.693(3)	11.635(3)	11.565(3)	11.518(3)	11.440(3)	11.845(3)	11.772(3)
Fe···Fe[g]	9.526(2)	9.532(2)	9.548(2)	9.561(2)	9.530(2)	9.490(2)	9.860(2)	9.847(2)
N14···N14[c]	9.051(6)	9.013(6)	8.989(5)	8.950(5)	8.950(5)	8.960(5)	9.034(4)	8.961(3)
N4···N4[d]	9.974(8)	9.962(8)	9.943(8)	9.948(8)	9.943(7)	9.938(8)	9.610(7)	9.475(6)
N12···N12[c]	6.652(6)	6.628(5)	6.615(5)	6.594(5)	6.600(5)	6.624(7)	6.677(4)	6.636(3)
N2···N2[d]	7.428(7)	7.435(6)	7.424(6)	7.419(6)	7.422(6)	7.439(8)	6.973(5)	6.852(4)
Fe···Cl	5.815(4)	5.810(4)	5.801(4)	5.792(4)	5.758(4)	5.716(4)	5.295(4)	5.240(4)

[a] X = N for **2** and X = O for **3**. Symmetry operations as indicated in the footnotes below. [b] −x+1, −y, −z+1. [c] −x+1, −y, −z. [d] −x, −y+1, −z. [e] −1+x, 1+y, −1+z. [f] x, y, −1+z. [g] 1+x, y, z.

prepared in the reaction of **hbtz** with Fe(ClO$_4$)$_2$·6H$_2$O performed in acetonitrile. Contrary to the complex {[Fe-(**12pbtzOH**)$_2$(CH$_3$CN)$_2$](ClO$_4$)$_2$·2CH$_3$CN}$_\infty$ crystallizing in the presence of an excess of iron(II) salt, the synthesis of **2** proceeds in the **hbtz**: Fe(II) molar ratio 2:1. A reaction performed between **hbtz** and Fe(II) in the molar ratio 3:1 also leads to formation of the same product **2**. A synthesis carried out in ethanol instead of acetonitrile afforded complex {[Fe(**hbtz**)$_2$(C$_2$H$_5$OH)$_2$](ClO$_4$)$_2$}$_\infty$ (**3**). Also in this case product stoichiometry is independent of the ligand to the metal ion ratio used in the reaction. **2** and **3** have grown as colorless crystals, stable in the nitrogen atmosphere.

We have noticed that similarly to the iron(II) complexes with 1-alkyl tetrazoles and 4-alkyl-1,2,4-triazoles also the cooling of the sample of **2** in liquid nitrogen is accompanied by a thermochromic effect. An observed pronounced change of color from white to purple indicates the HS→LS transition. No color changes in the cooling of the sample of **3** was noticed.

Results of Magnetic Susceptibility Measurements of 2 and 3. The temperature dependent magnetic susceptibility measurements for both complexes were carried out over the 5−300 K range (Figure 1). An observed $\chi_M T$ (χ_M-molar susceptibility, T-temperature) value at 300 K of 3.4 cm^3 K/mol is characteristic for a high spin form of iron(II) ion. In the temperature threshold of 300−200 K the $\chi_M T$ value slightly increases. Further lowering of the temperature involves a gradual lowering of the $\chi_M T$. In the range of 150−120 K the $\chi_M T$ value decreases more abrupt ($T_{1/2}{}^\downarrow$ = 128 K).

Below 120 K the $\chi_M T$ decreases gradually reaching at 75 K the value of 0.30 cm^3 K/mol which confirms the HS→LS transition. In the warming mode the course of the $\chi_M T(T)$ dependency is the same as it was observed in

the cooling cycle. This behavior indicates an absence of a thermal hysteresis loop. Results of magnetic measurements show that between 150 (γ_{HS} = 0.80) and 120 K (γ_{HS} = 0.20) about 60% of iron(II) ions change their spin state.

3 is paramagnetic in the whole temperature range. Between 300 and 50 K the $\chi_M T$ is almost constant and equal to 3.4 cm^3 K/mol. The lowering of the $\chi_M T$ value below 25 K may be attributed to the zero-field splitting of the high spin iron(II) ions.

Structural Studies of 2 and 3. Crystal structures at 293, 250, 200, 150, 125, and 100 K for **2** and at 250 and 100 K for **3** were determined. Both complexes crystallize in $P\overline{1}$ space group, and they are isostructural. An asymmetric part of the unit cells consist of an iron(II) ion located on the special position, solvent (acetonitrile in **2** or ethanol in **3**), and two **hbtz** molecules as well as a perchlorate anion (Figure 2). The first coordination spheres of iron-(II) in **2** and **3** are composed of four tetrazole rings and two molecules of the suitable solvent. 2-Substituted tetrazoles coordinate monodentately through N4 and N14 nitrogen atoms of the rings, and they form basal plane of the coordination octahedron.

In **2** at 293 K the Fe−N4 and Fe−N14 bond lengths are equal to 2.166(3) and 2.189(3) Å, respectively. These values are similar to that ones found in the high spin form of the complex {[Fe(**pbtz**)$_3$](ClO$_4$)$_2$·2EtOH}$_\infty$[11] (where **pbtz** = 1,3-di(tetrazol-2-yl)propane) and they are slightly shorter than Fe−N4 distances in {[Fe(**pbtz**)$_3$]-(ClO$_4$)$_2$}$_\infty$[11] which does not exhibit the HS⇆LS transition. The apical positions in **2** are occupied by symmetry related acetonitrile molecules. The Fe−N100 distance is equal to 2.162(4) Å. This bond length is comparable to the Fe(HS)-N(CH$_3$CN) distances in the complex based on
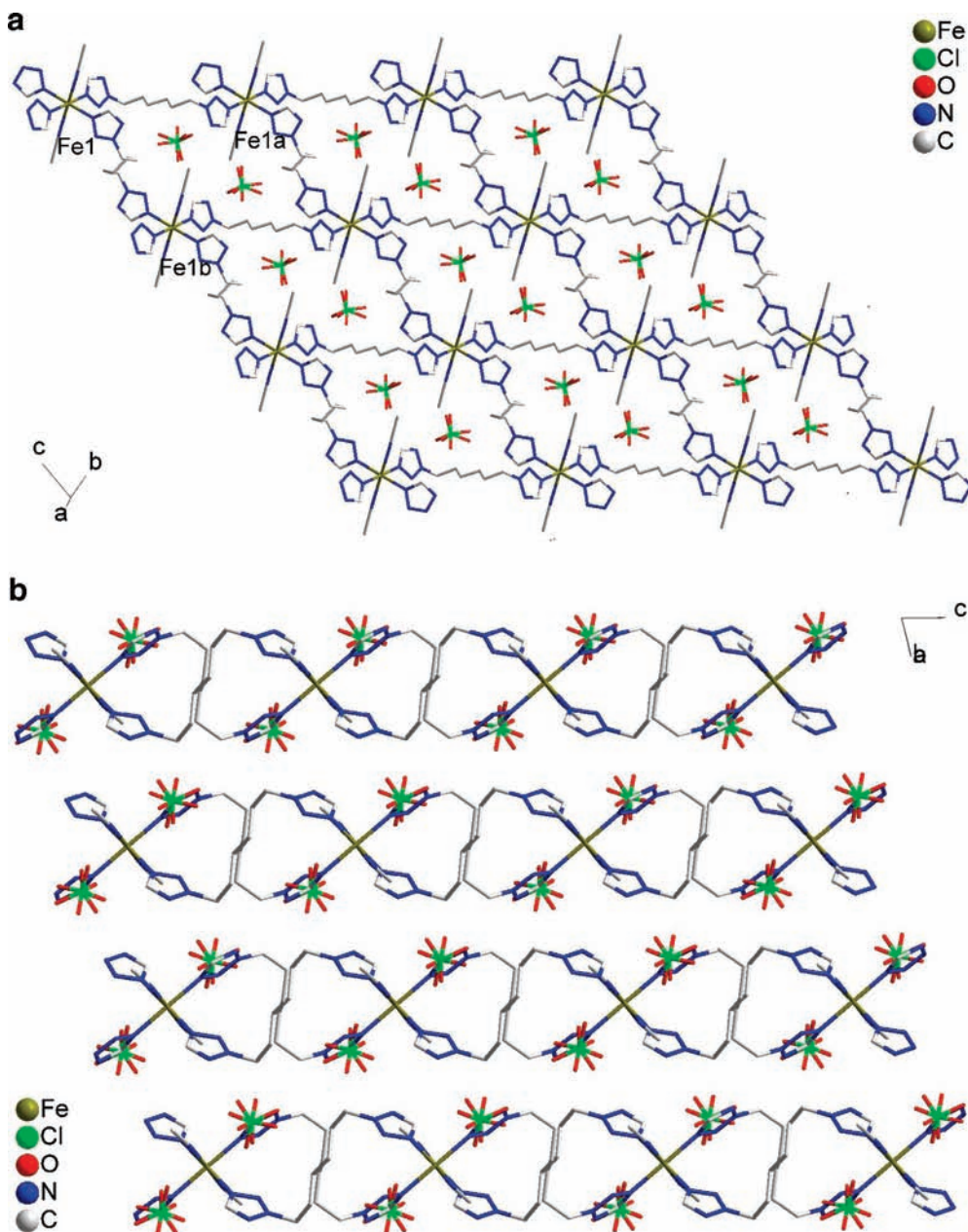
Figure 3. View of (a) a single polymeric layer, (b) a packing of 2D layers in **2**. Symmetry operations: a = −1 + x, 1 + y, −1 + z; b = x, y, −1 + z.

mixed ligand systems[24] and in hexakis(acetonitrile)iron-(II) hexafluoroantimonate.[25] The N−Fe−N angles range from 88.0(1) to 92.0(1)° (see Table 2).

The geometry of the FeN$_6$ chromophore at 293 K is characteristic for the high spin form of the iron(II) ion and remains practically the same during cooling to 200 K. At 150 K the average Fe−N distances are slightly shortened indicating a beginning of the HS→LS transition which is in agreement with the results of the magnetic studies. Further lowering of temperature below 150 K involves more abrupt alterations of the crystal structure parameters. At 125 K, the average Fe−N4, Fe−N14, and

Fe−N100 distances are equal to 2.080(3), 2.094(3), and 2.061(3) Å, respectively. This shortening of the Fe−N distances corresponds to a random distribution of high spin and low spin iron(II) ions in the same crystallographic site. The Fe−N distances at 125 K manifest an approximately equal amount of high and low spin iron(II) which corresponds to the magnetic studies. After cooling to 100 K, the Fe−N4 and Fe−N14 distances are equal to 2.000(3) and 2.011(3) Å, respectively. Shortening of the Fe−N(tetrazol) bond lengths at 0.17 and 0.18 Å in **2**, induced by temperature lowering from 293 to 100 K, is slightly greater than ones observed for {[Fe(**pbtz**)$_3$]-(ClO$_4$)$_2$·2EtOH}$_∞$[11] and {[Fe(**12pbtzOH**)$_2$(CH$_3$CN)$_2$]-(ClO$_4$)$_2$·2CH$_3$CN}$_∞$[14] because of incomplete spin transitions at 100 K in these two complexes. The changes of the Fe−N bond lengths in **2** are similar to those ranging from 0.16 to 0.20 Å that occurred for the complete spin transition

(24) Edwards, P. G.; Harrison, A.; Newman, P. D.; Zhang, W. *Inorg. Chim. Acta* **2006**, *359*, 3549–3556.

(25) Brennessel, W. W.; Brooks, N. R.; Mehn, Que, M. P. L., Jr.; Young, V. G., Jr. *Acta Crystallogr.* **2001**, *E57*, m545–m546.
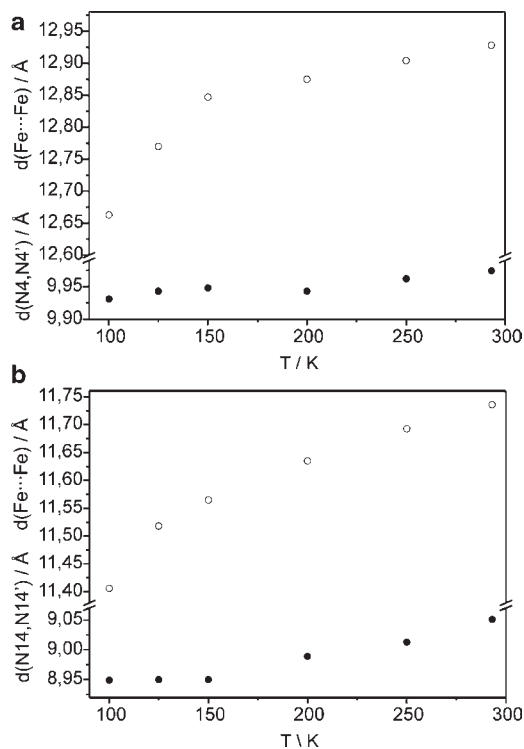
Figure 4. Temperature dependency of intralayer Fe···Fe (open circles) and N4,N4′ (filled circles) distances in the [1$\bar{1}$1] (a) and [001] (b) directions in **2**.

Figure 5. Superpositions showing conformations of ligand bridges in **3** (red, green) in relation to **2** (blue) at 250 K in the (a) [1$\bar{1}$1] and (b) [001] directions. Green color denotes the conformer of **hbtz** occupying at 250 K 20% of the second alternative position which is not observed after cooling to 100 K.

in complexes of iron(II) with 1-substituted tetrazoles.[7,9a,26] In **2** at 100 K the Fe−N100(CH_3CN) bond length is equal to 1.953(3) Å. In this case contraction of the bond length at 0.21 Å is also greater than the one found for {[Fe(**12pbtzOH**)$_2$-(CH_3CN)$_2$](ClO$_4$)$_2$·2CH$_3$CN}$_\infty$. In the low spin form of iron(II) complexes with chromophores FeN$_6$, the Fe−N(CH_3CN) distances lie in the range 1.93−1.95 Å.[27] Thus, the shortening of the Fe−N distances in **2** upon lowering of temperature confirms the HS→LS transition. After the spin transition, the geometry of the FeN$_6$ chromophore stays the same (Table 2). The Σ values at 250 and 100 K are equal to 11.5° and 11.1°, respectively.

The parameters of the FeN$_4$O$_2$ chromophore in **3** are characteristic for the high spin(II) form of iron(II) ion, and the geometry of the coordination octahedron remains unchanged after lowering of the temperature to 100 K (Table 2).

The two crystallographically unrelated **hbtz** molecules in **2** differ from each other in their conformations. Both conformers bridge iron(II) ions in different directions. An alkyl spacer of **hbtz** molecules linking iron(II) ions in the [1$\bar{1}$1] direction adopts an extended zigzag conformation. The tetrazole rings are *transoidal* oriented, the distance between the N4···N4(−x, 1−y, −z) donor atoms at 293 K is equal to 9.974(8) Å, and the distance between iron(II) ions in the [1$\bar{1}$1] bridging direction equals 12.928(8) Å. In the other crystallographically unrelated **hbtz** molecule, *transoidal* oriented tetrazole rings are tethered by a hexyl
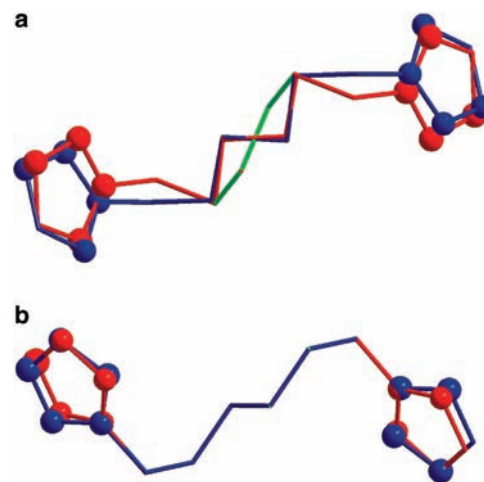
spacer adopting S-shaped conformation. Here the N14···N14(1−x, −y, −z) distance is equal to 9.051(6) Å. The S-shaped ligand molecule links iron(II) ions arranged in the [001] direction separating them at the distance of 11.736(3) Å. In effect, cross-linking of the iron(II) ions gathered in a common plane involves the formation of a 2D layer with a grid-like pattern (Figure 3).

A comparison of torsion angles of both crystallographically unrelated **hbtz** molecules in **2** points out that diversification of the distances between iron(II) ions, bridged in the [1$\bar{1}$1] and in the [001] directions, results from various conformations of ligands. The conformational versatility originates mainly from a rotation around the C2−C3 bond of the hexane spacer (see Table 2).

The Fe···Fe separations in **2** belong to the shortest ones observed in the coordination polymers based on ligand systems composed of N-substituted azole rings linked by the hexane spacer. In complexes of divalent transition metal ions with 1,6-di(imidazol-1-yl)hexane[28] and 1,6-di(1,2,4-triazol-1-yl)hexane[29] metal ions are separated at distances ranging from 13.7 to 16.1 Å and from 14.3 to 16.9 Å, respectively. It is worth emphasizing that the distances between iron(II) atoms observed in **2** at 293 K (12.9 and 11.7 Å) are also shorter than distances between high spin iron(II) ions linked by 1,4-di(tetrazol-1-yl)butane[9a,b] and 1,4-di(1,2,4-triazol-1-yl)butane[30] (14.4 and 13.9 Å, respectively) and comparable to the ones observed for 1,4-di(1,2,3-triazol-1-yl)butane (11.7 Å).[31]

Between 293 and 150 K a gradual lowering of the Fe···Fe distances along the bridging directions takes place (Figure 4). In this temperature threshold also a

(26) (a) Kusz, J.; Spiering, H.; Gutlich, P. *J. Appl. Crystallogr.* **2001**, *34*, 229–238. (b) Kusz, J.; Spiering, H.; Gutlich, P. *J. Appl. Crystallogr.* **2004**, *37*, 589–595.

(27) Diebold, A.; Hagen, K. S. *Inorg. Chem.* **1998**, *37*, 215–223.

(28) (a) Qi, Y.; Luo, F.; Che, Y.; Zheng, J. *Cryst. Growth Des.* **2008**, *8*, 606–611. (b) Zhang, W.-L.; Liu, Y.-Y.; Ma, J.-F.; Jiang, H.; Yang, J.; Ping, G.-J. *Cryst. Growth Des.* **2008**, *8*, 1250–1256.

(29) Liu, Y.-Y.; Yi, L.; Ding, B.; Huang, Y.-Q.; Cheng, P. *Inorg. Chem. Commun.* **2007**, *10*, 517–519.

(30) Gu, Z.-G.; Xu, Y.-F.; Zhou, X.-H.; Zuo, J.-L.; You, X.-Z. *Cryst. Growth Des.* **2008**, *8*, 1306–1312.

(31) Bronisz, R. *Inorg. Chem.* **2005**, *44*, 4463–4465.

Table 3. Selected Interatomic Contacts [Å] and Angles [deg] for **2** at 293, 250, 200, 150, 125, and 100 K and for **3** at 250 and 100 K[a]

	293 K		250 K		200 K		150 K		125 K		100 K	
	D···A	D–H···A	D···A	D–H···A	D···A	D–H···A	D···A	D–H···A	D···A	D–H···A	D···A	D–H···A
Compound **2**												
C11–H11E···O3[b]	3.178(12)	122	3.135(9)	122	3.154(7)	120	3.157(4)	119	3.161(4)	118	3.169(4)	118
C11–H11D···O2[c]	3.478(10)	166	3.501(13)	162	3.505(5)	165	3.522(4)	164	3.510(4)	164	3.473(4)	165
C4–H4···O1[d]	3.100(11)	149	3.124(14)	147	3.104(6)	147	3.110(4)	146	3.099(4)	144	3.091(4)	141
C1–H1A...O1[e]	3.214(12)	114	3.170(12)	112	3.233(6)	114	3.225(4)	114	3.207(4)	115	3.185(4)	116
C12–H12...O3[f]	3.399(10)	121	3.429(11)	119	3.420(5)	120	3.426(4)	120	3.416(4)	121	3.398(4)	122
C14–H14···O3[g]	3.273(12)	138	3.303(13)	135	3.277(6)	134	3.271(4)	133	3.236(4)	132	3.197(4)	130
C14–H14···O4[g]	3.307(11)	138	3.341(16)	144	3.307(8)	142	3.297(4)	144	3.279(4)	144	3.242(4)	143
C110–H11A···O1	3.405(12)	133	3.361(13)	129	3.330(6)	153	3.330(5)	154	3.332(4)	154	3.338(5)	154
Compound **3**												
O100–H100···O4			2.764(3)	174							2.733(3)	173
C4–H4···O1[d]			3.27(3)	144							3.329(2)	154
C4–H4···O21[d]			3.281(8)	156								
C11–H11A···O2[c]			3.09(3)	150								
C11–H11B···O2[b]											3.367(2)	144
C14–H14···O3[g]			3.18(3)	136							3.393(3)	154

[a] Symmetry operations as indicated in the footnotes below. [b] x, $1+y$, $-1+z$. [c] $2-x$, $-1-y$, $1-z$. [d] $-1+x$, $1+y$, z. [e] $1-x$, $-1-y$, $1-z$. [f] x, $1+y$, $-1+z$. [g] $1-x$, $-y$, $1-z$.

shortening of the distances between the N4 and N4($-x$, $1-y$, $-z$) as well as between the N14 and N14($1-x$, $-y$, $-z$) donor atoms of the ligand molecules (iron(II) ions are bridged in the [1$\bar{1}$1] and [001] directions, respectively) takes place. Below 150 K the shortening of the Fe···Fe separations in the [1$\bar{1}$1] and [001] directions proceeds more steeply. Simultaneously, a slight reduction of N4···N4($-x$, $1-y$, $-z$) distance still takes place and is accompanied by the alteration of N2–C1–C2–C3 torsion angle (Table 2). The N14···N14($1-x$, $-y$, $-z$) distance is practically the same below this temperature. At 100 K in the low spin form of **2**, the distances between iron(II) ions bridged in the [1$\bar{1}$1] and [001] directions are markedly shortened to 12.663(8) Å and 11.440(3)Å, that is, at 0.24 and 0.25 Å in relation to 250 K, respectively. This behavior is common for polymeric spin crossover complexes in which the spin transition usually involves the compression of the crystal lattice along the bridging direction of the iron(II) ions. After the spin transition in **2**, distances between nitrogen donor atoms of ligand molecules forming bridges in the [1$\bar{1}$1] and [001] directions are shortened to 9.938(8) and 8.960(7)Å, respectively. In other iron(II) complexes with bistetrazole-type ligands observed alterations of distances between nitrogen donor atoms range from −0.05 to 0.03 Å. Thus, shortening of the N4···N4($-x$, $1-y$, $-z$) and N14···N14($1-x$, $-y$, $-z$) distances at about 0.04 and 0.09 Å in **2** indicates a relatively great elasticity[32] of the ligand molecules possessing a long alkyl spacer. Conformational analysis indicates that subtle changes of ligand conformations, depending on combination of rotation of the tetrazole rings in relation to the alkyl chain and changes of the torsion angles of the alkyl chains, are responsible for the observed alterations in **2** (see Table 2).

On the contrary to **2**, one of the crystallographically unrelated **hbtz** molecules in **3** reveals disorder over two positions (atoms C3–C3($-x$, $1-y$, $-z$) or C31–C31($-x$,

$1-y$, $-z$)) with occupancies 0.8/0.2 at 250 K (Figure 5). Disordered **hbtz** ligand molecules bridging iron(II) ions in the [1$\bar{1}$1] direction separate them at a distance of 12.687(8) Å, which is reduced to 12.546 (8) Å, that is, at 0.14 Å at 100 K. After lowering of the temperature, the distances between N4···N4 ($-x$, $1-y$, $-z$) and N2···N2 ($-x$, $1-y$, $-z$) atoms are shortened at 0.14 Å and 0.12 Å, respectively, indicating the strong influence of the spacer conformation. At 100 K only the conformer dominating at 250 K is present. Similarly like in **2**, iron(II) ions arranged in the [001] direction are bridged by ordered **hbtz** ligand molecules. In this bridging direction the Fe···Fe (x, y, $1+z$) distance at 250 K is equal to 11.845(3) Å and at 100 K it decreases to 11.772(3) Å, that is, at 0.09 Å. After lowering of temperature from 250 to 100 K the N14···N14 ($1-x$, $-y$, $-z$) and N12···N12 ($1-x$, $-y$, $-z$) distances are reduced at about 0.07 and 0.04 Å, respectively. Conformational analysis of the second type of bridge in **3** reveals that in this case the elasticity of the ligand molecules is responsible for the reduction of the Fe···Fe(x, y, $1+z$) distance. To sum up, the alterations of the Fe···Fe intralayer separations in **3** proceed, contrary to **2**, in two different ways resulting in substantial diversification of compressions in both bridging directions.

The perchlorate anions in **2** are gathered in the peripheries of the 2D layers in the vicinity of the coordination octahedrons. In the high spin form they are disordered over two positions with occupancy factor equal to 0.6/0.4. Upon lowering of temperature the occupancy factor of the major component gradually increases. At 100 K the disorder of the perchlorate anions over two positions is maintained, and the occupancy factor is equal to about 0.9/0.1. This behavior suggests a low crystal packing efficiency because neither the compression caused by decreasing of the temperature nor the spin transition forces a vanishing of orientational disorder of the perchlorate anions. The shortest distance Fe···Cl(ClO$_4$⁻) (x, y, z) at 293 K is equal to 5.815(4)Å and is reduced in the

(32) Comba, P.; Schiek, W. *Coord. Chem. Rev.* **2003**, *238−239*, 21–29.

low spin form to 5.716(4)Å. The perchlorate anion is engaged in the formation of distant contacts within the layer (see Table 3). After cooling, the number of intermolecular contacts stays the same; however, three contacts, that is, C14−H14···O3(ClO$_4^-$) (1−x, −y, 1−z), C14−H14···O4(ClO$_4^-$) (1−x, −y, 1−z) and C110−H11A···O1-(ClO$_4^-$) are slightly shorter.

In **3**, perchlorate anions reveal severe disorder at 250 K but, in contrast to **2**, they are ordered at 100 K. Anions are engaged in the formation of O−H···O(ClO$_4^-$) hydrogen bonds with coordinated ethanol molecules (see Table 3).

There are no significant interactions between the parallel oriented 2D layers in **2** (Figure 3b). The shortest interlayer Fe···Fe (1+x, y, z) distance at 293 K is equal to 9.526(2) Å. A consequence of the lowering of temperature from 293 to 150 K is an increase of the distance between iron atoms from the neighboring layers, contrary to the alterations of the Fe···Fe intralayer separations. This tendency undergoes an inversion after reaching of 150 K and an abrupt decrease of the interlayer Fe···Fe (1+x, y, z) separation occurs. The shortest Fe···Fe(1+x, y, z) interlayer separation at 100 K is equal to 9.490(2) Å. The direction of this change is comparable to that ones found for 1D systems and interpenetrated 3D coordination networks based on bis(tetrazol-1-yl)alkanes. On the other hand this alteration proceeds in an opposite direction in relation to the 2D system {[Fe(btr)$_2$(SCN)$_2$]·H$_2$O}$_\infty$ in which an abrupt spin transition involves an increase of the interlayer distance.[33]

In **3**, similarly like in **2**, there is a lack of direct significant interactions between the parallel oriented 2D layers, and after lowering of temperature from 250 to 100 K the Fe···Fe (1+x, y, z) interlayer separation is reduced at about 0.01 Å (see Table 2).

Conclusions

The reactions described in this paper between 1,6-di-(tetrazol-2-yl)hexane and iron(II) perchlorate hexahydrate carried out in the ligating solvents (acetonitrile or ethanole) afforded heteroleptic complexes of formula {[Fe(**hbtz**)$_2$-(solv)$_2$](ClO$_4$)$_2$}$_\infty$ (solv = acetonitrile or ethanol). Previously we have reported another heteroleptic system {[Fe(**12pbtzOH**)$_2$-(CH$_3$CN)$_2$](ClO$_4$)$_2$·2CH$_3$CN}$_\infty$ (**12pbtzOH** = 2-hydroxy-1-(tetrazol-1-yl)-3-(tetrazol-2-yl)propane)[14] in which the first

coordination sphere is composed of both N-substituted regioisomers of tetrazole. On the other hand, it is known that in the absence of coordinating anions, mono 1-substituted tetrazoles reacting with iron(II) salts tend in general toward formation of homoleptic complexes in which iron(II) ions are coordinated with six tetrazole rings.[7−10,34] Thus, in comparison with their tetrazol-1-yl analogues, coordination behavior of **hbtz** indicates a greater inclination of bis(tetrazol-2-yl)-type ligands to produce iron(II) systems containing a Fe(tetrazol)$_4$-(CH$_3$CN)$_2$-type core.

Differences in the chemical compositions between **2** and **3** have profound consequences for their magnetic properties. The complex **3** possessing a FeN$_4$O$_2$ chromophore is paramagnetic in the range of 5−300 K whereas **2** exhibits the spin transition.

Complexes **2** and **3** are isostructural. In both compounds, iron(II) ions are bridged in two directions (i.e., [1$\bar{1}$1] and [001]) giving a coordination network with (4,4) topology. In **2**, apart from reduction of the Fe−N bond lengths, the HS→LS transition involves also a shortening of the distances between iron(II) ions and N4,N4′ donor atoms of **hbtz** molecules in both bridging directions. In **2** and **3**, ligand molecules arranged in the [001] direction exhibit very similar conformation, and upon lowering of temperature distances between N4,N4′ donor atoms are shortened to a similar value. For a change, iron(II) ions in **3** are bridged in the [1$\bar{1}$1] direction by ligands adopting two different conformations, whereas in **2** disordering of **hbtz** molecules is not observed. In relation to **2**, lowering of the temperature in **3** causes disappearance of ligand disorder and significantly greater shortening of the N4,N4′ separation. Comparison of both types of ligand bridges reveals greater susceptibility to alteration of geometrical parameters in that one which is composed of conformationally labile molecules.

To sum up, in the investigated complexes, we have noticed manifestations of both elasticity and flexibility of the ligand molecules. In **2**, in the absence of the strong interactions between 2D layers, the elasticity of the bridging ligand molecules and the low crystal packing seem responsible for a relatively gradual spin transition.

(33) Legrand, V.; Pillet, S.; Carbonera, C.; Souhassou, M.; Letard, J.-F.; Guionneau, P.; Lecomte, C. *Eur. J. Inorg. Chem.* **2007**, 5693–5706.
(34) Absmeier, A.; Bartel, M.; Carbonera, C.; Jameson, G. N. L.; Weinberger, P.; Caneschi, A.; Mereiter, K.; Letard, J.-F.; Linert, W. *Chem.—Eur. J.* **2006**, *12*, 2235–2243.